Supplementary Materials

High open-circuit voltage in single-crystalline n-type SnS/MoO_3 photovoltaics

Issei Suzuki[1,*], Zexin Lin[1], Taichi Nogami[1], Sakiko Kawanishi[1],
Binxiang Huang[2], Andreas Klein[2], Takahisa Omata[1]

1. Institute of Multidisciplinary Research for Advanced Materials (IMRAM), Tohoku University, 2-1-1 Katahira, Aoba-ku, Sendai 980-8577, Japan
2. Department of Materials and Earth Science, Electronic Structure of Materials, Technical University of Darmstadt, Otto-Berndt-Str. 3, 64287 Darmstadt, Germany.

*Corresponding author E-mail address: issei.suzuki@tohoku.ac.jp

Supplementary Note.1
Valence state of Mo in MoO_3 thin films

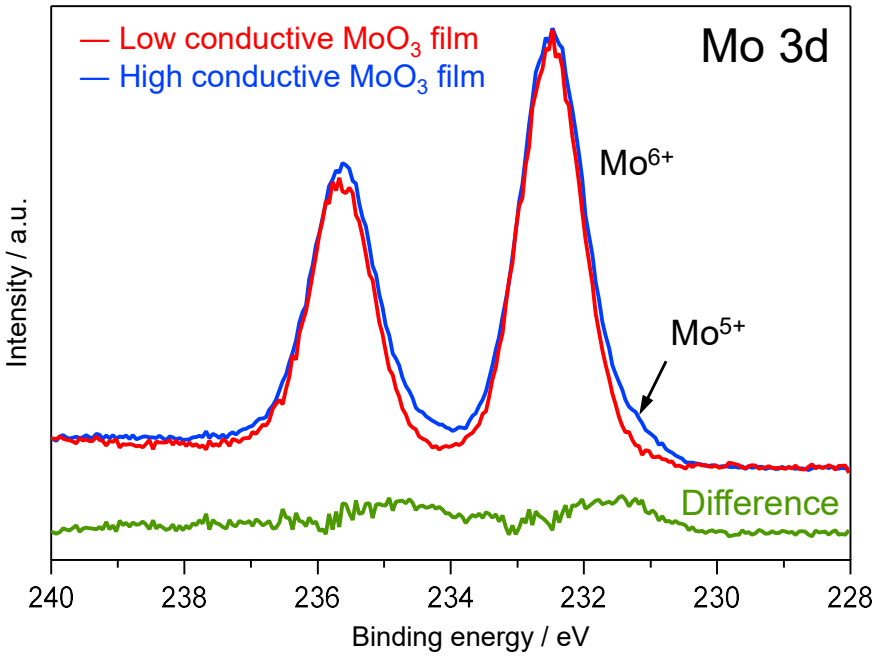

FIG. S1. XPS spectra of the surfaces of low- and high-conductivity MoO_3 thin films (red and blue lines, respectively), which were deposited onto glass substrates. The green line shows the difference. The spectra were aligned with the main peaks at 232.5 eV. Only the spectrum of the high-conductivity MoO_3 layer exhibited a shoulder band at a lower binding energy. This may be owing to the introduction of oxygen vacancies resulting in the partial reduction of Mo^{6+} to Mo^{5+}. The chemical shift of Mo^{6+} and Mo^{5+} is reported to be ~1 eV[S1], which is consistent with the observed energy difference between the main and shoulder peaks (green line). Notably, the thin films were exposed to air prior to the XPS measurement; therefore, the spectra may be partially affected by surface contamination and/or possible reaction with air.

Supplementary Note.2
MoO_3 thickness dependence of the photovoltaic properties

The effects of MoO_3 thickness on the photovoltaic properties and device parameters are shown in Fig. S2, and those of the device with the highest *PCE* are summarized in Table S1. High V_{OC} values were obtained when the MoO_3 layer thickness was 3 and 6 nm, and V_{OC} decreased when the MoO_3 layer thickness was 1.5 and 12 nm (Fig. S2(a)). It is assumed that the 1.5-nm-thick MoO_3 layer is too thin to form an inadequate interface, and thus the V_{OC} becomes lower, considering that the band bending at the interface of n-type SnS with MoO_3 becomes complete when the MoO_3 layer is more than ~3 nm[S1]. The devices with a 12-nm-thick MoO_3 layer exhibited a reverse saturation current (J_0), which was larger than those of devices fabricated with other MoO_3 layer thicknesses (Fig. S2(g)). This indicates a high recombination rate at the interface, suggesting that a thicker MoO_3 layer does not allow efficient carrier separation, resulting in a lower V_{OC}. Moreover, J_{sc} and FF exhibited no clear relationship with MoO_3 thickness (Fig. S2(b,c)). Thus, the MoO_3 layer thickness dependence of *PCE* reflects that of V_{OC}. Thus, the 3- and 6-nm-thick MoO_3 layers are favorable for both V_{OC} and *PCE* (Fig. S2(a,d)).

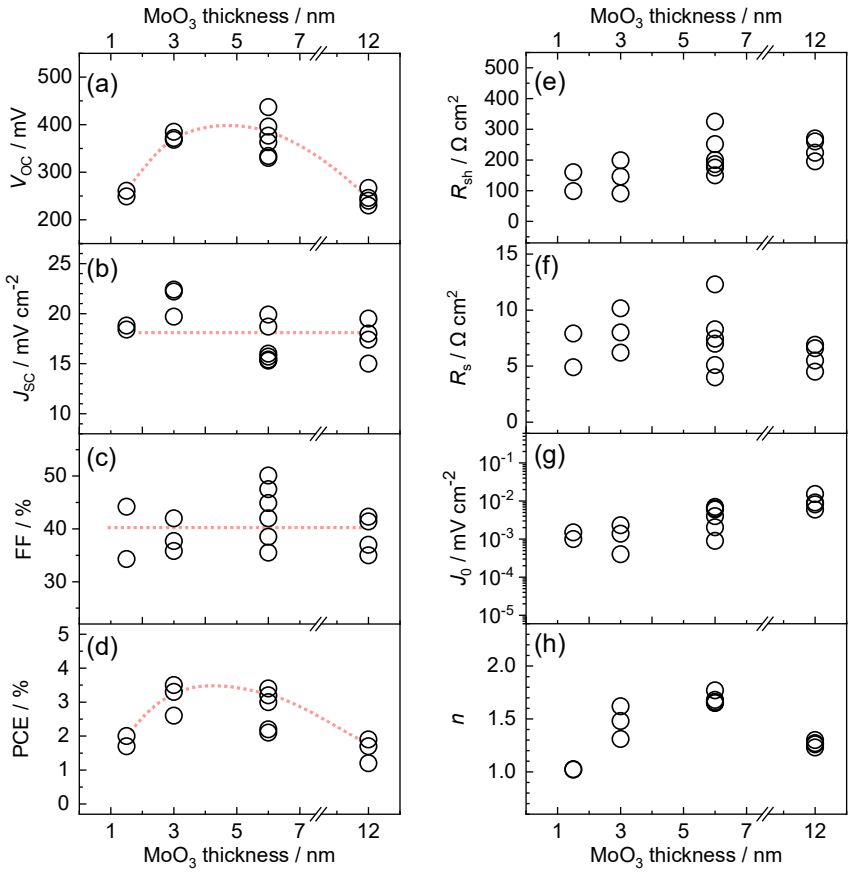

FIG. S2. Photovoltaic performance of n-type SnS single crystal/MoO_3 junction solar cells as a function of MoO_3 thickness. The MoO_3 layer with a low conductivity (σ_{MoO_3} = 1.7×10^{-8} Scm^{-1}) was used. (a) V_{OC}, (b) J_{SC}, (c) *FF*, (d) *PCE*, (e) R_{sh}, (f) R_s, (g) J_0, and (h) *n*. Dotted lines are only for eye guides.

Table S1. Photovoltaic characteristics of representative solar cells with n-type SnS single crystal/MoO_3 junctions with different MoO_3 layer thicknesses and conductivities.

MoO_3 layer conductivity	MoO_3 layer thickness	*PCE* / %	V_{OC} / mV	J_{SC} / mA cm^{-2}	FF / %	R_{sh} / Ω cm^2	R_s/ Ω cm^2	J_0 / mA cm^{-2}	*n*
Low σ_{MoO_3} (1.7×10^{-8} S cm^{-1})	1.5 nm	2.0	249	18.4	44.2	160	4.9	1.5×10^{-3}	1.02
	3 nm	3.3	385	22.4	37.7	146	8.0	2.3×10^{-3}	1.48
	6 nm	3.4	437	15.7	50.1	200	7.5	9.0×10^{-4}	1.77
	12 nm	1.9	246	19.1	42.3	270	4.5	9.2×10^{-3}	1.26

Supplementary Note.3
EQE spectra

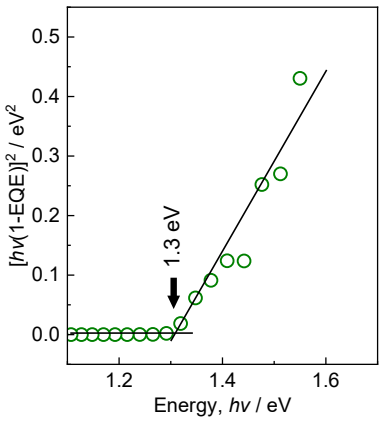

FIG. S3. Bandgap of the absorber layer determined by the plot of [*hv*(1-EQE)]^2 against *hv*. The device is fabricated using 6-nm-thick MoO_3 thin films with a high σ_{MoO_3}.

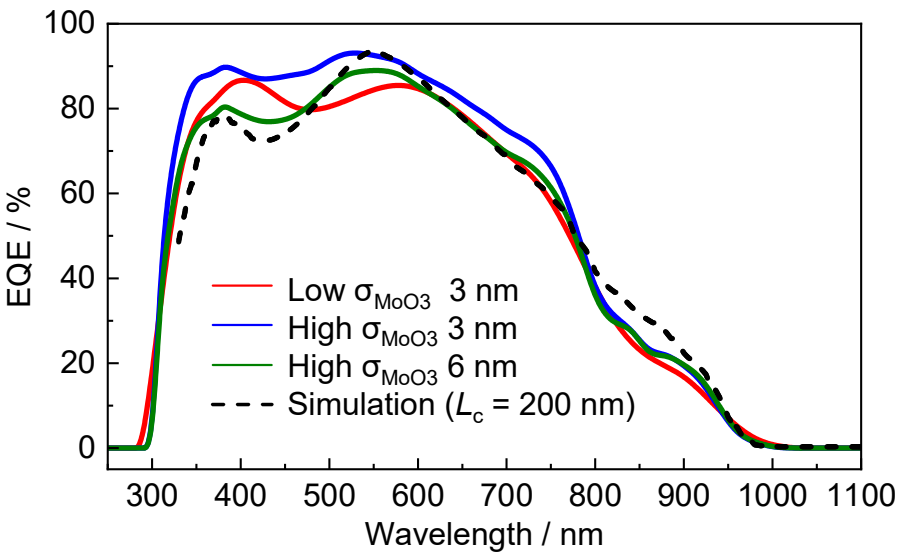

FIG. S4. EQE spectra of the solar cells with n-type SnS single crystal/MoO_3 film junctions with different MoO_3 layer thicknesses and conductivities. The simulated spectrum is obtained by EQE using the e-ARC code.

REFERENCES

[S1] I. Suzuki, B. Huang, S. Kawanishi, T. Omata, A. Klein, Avoiding Fermi Level Pinning at the SnS Interface for High Open-Circuit Voltage, J. Phys. Chem. C. 126 (2022) 20570–20576.